J. Appl. Comput. Mech., 9(4) (2023) 935-944
DOI: 10.22055/jacm.2023.42743.3969

ISSN: 2383-4536
jacm.scu.ac.ir

Shahid Chamran University of Ahvaz

Journal of Applied and Computational Mechanics

Research Paper

Delamination Analysis of Multilayered Functionally Graded Beams which Exhibit Non-linear Creep Behavior

Victor Rizov

Department of Technical Mechanics, University of Architecture, Civil Engineering and Geodesy, 1 Chr. Smirnensky blvd., Sofia - 1046, Bulgaria

Received January 10 2023; Revised March 08 2023; Accepted for publication March 09 2023.
Corresponding author: V. Rizov (V_RIZOV_FHE@UACG.BG)

Abstract. General solution of the time-dependent strain energy release rate for delamination cracks in multilayered functionally graded load-bearing beam structures which exhibit non-linear creep is derived. The material is functionally graded along the length of layers. The Ramberg-Osgood stress-strain relation is used by assuming that the material in each layer behaves differently in tension and compression. The second term in the Ramberg-Osgood relation includes time dependence to treat the non-linear creep. The solution derived holds for multilayered functionally graded beams with arbitrary number of layers which have different width and material properties. The solution is applied for a delamination in a multilayered beam with a built-in end. An analysis is performed also by considering the balance of the energy in the multilayered beam configuration for the sake of verification. The effect of time is also studied. It is found that the strain energy release rate grows with the time. The results obtained here are useful for understanding the time-dependent delamination in multilayered functionally graded structural components subjected to non-linear creep.

Keywords: Beam, Functionally graded material, Multilayered structure, Material non-linearity, Fracture, Time-dependent behaviour.

1. Introduction

The most important feature of functionally graded engineering materials is that their properties vary smoothly in the volume of solid [1-5]. In fact, these materials are made of several phases [6-11]. One of the advantages of these materials over the homogeneous engineering materials is the possibility the properties of functionally graded materials to be formed technologically [12-17]. Also, since the material properties vary smoothly without sudden changes, the risk of failure from interfacial stress concentrations is significantly reduced.

Multilayered engineering materials refer to inhomogeneous materials which consist of layers of dissimilar materials. The interest towards the multilayered inhomogeneous engineering structures is due mainly to the fact that they have higher strength-to-weight and stiffness-to-weight ratios compared to the homogeneous structures. Thus, the multilayered materials are very suitable for use in various light-weight load-carrying structural applications. As the use of multilayered materials increases, the requirements for integrity, reliability and durability of multilayered engineering structures increases too.

The major treat to the integrity of multilayered inhomogeneous structures is the delamination fracture. Delamination, or separation of layers, reduces the strength and stiffness and affects the performance and safety of multilayered structures. Therefore, delamination problems of multilayered materials and structures are an important subject of research [18-22]. It is known that the strain energy release rate (SERR) is the driving force of delamination in multilayered structural components. This circumstance underlines the significance of deriving of SERR solutions for various delamination problems. Useful delamination analysis of a multilayered beam configuration is presented in [21]. The beam under consideration is bended transversely to the layers. A notch is cut on the upper surface of the beam in the mid-span such that the upper delamination arm is free of stresses. The strain energy stored in the beam as a result of bending is analyzed in order to obtain the SERR for the delamination crack. The solution found in [21] expresses the SERR as a function of the lower delamination arm thickness, the bending moment, the layer number, the thickness and the modulus of elasticity of layers (the case of a multilayer beam structure made of layers of different materials is considered in [21]). Various aspects of delamination problem are extensively researched in [22]. Useful solutions of the SERR for delamination in different load-carrying beam-like engineering structures subjected to static bending transversely to the layers are obtained and thoroughly discussed. The problems of delamination behaviour of beams in which the delamination arms have different thickness are successfully tackled in [22]. Longitudinal cracks in layers loaded along edges are also studied in [22]. It is shown that the SERR solutions derived can be applied also to deal with the problem of debonding of thin films [22].

The literature survey indicates that, usually, the delamination problem of multilayered structural components is treated by using concepts of linear-elastic fracture mechanics which are based on the hypothesis for linear nature of the constitutive stress-

Published online: March 19 2023

strain relationship. Multilayered components, however, may have also non-linear elastic behaviour. In such cases, delamination problem should be analyzed by taking into account the material non-linearity. This leads to indispensability of applying constitutive stress-strain relationships which have non-linear character.

Recently, delamination analyses of non-linear elastic multilayered beams by the Ramberg-Osgood relationship have been carried-out [23-25]. The analyses are focused on separate beam configurations [23-25]. Therefore, the main aim of the present paper is to develop general analysis of delamination in multilayered functionally graded beams by using the Ramberg-Osgood relation. The material is functionally graded along the length of the layers. General solution of the time-dependent strain energy release rate (TDSERR) is derived here assuming that the material behaves differently in tension and compression in contrast to [23-25] where it is assumed that the behavior of the multilayered material in tension and compression is identical. Besides, it is known that many load-carrying engineering structures have time-dependent behavior by reason of creep [27]. Therefore, time-dependent delamination induced by non-linear creep is analyzed here in contrast to previous paper [25] which is concerned with delamination under linear creep. A specific modification of the Ramberg-Osgood stress-strain relationship that is meant for treating of non-linear creep is used in the present paper. This modification is taken from Dowling's work [27].

2. General Solution of the TDSERR under Nonlinear Creep

In order to obtain the TDSERR, a portion of a multilayered functionally graded beam with the delamination crack front is considered (Fig. 1). The layers of the beam are made of different functionally graded materials. The beam is loaded in bending (the bending moment ahead of the delamination is M_3). The width and the height of the beam are b and h, respectively. The widths of the cross-sections of delamination arms 1 and 2 are denoted by b_1 and b_2. Concerning the loading of the beams, it should be specified that the beams studied in the present work are bent around the horizontal centric axis. In what follows, we will show that the TDSERR can be derived by considering only a beam portion with delamination front (Fig. 1) provided that the bending moments about the horizontal centric axis in sections ahead and behind the delamination front are known (these bending moments for a particular beam structure can be determined by analyzing the equilibrium of the beam). The solution derived here can be used to treat delamination in beam structures which supports are located so that the sections ahead and behind the delamination front are bent around the horizontal centric axis.

The behavior of the material in the tension and compression zones of i-th layer is treated by the Ramberg-Osgood relation written in the following form which is meant for treating of non-linear creep [27]:

$$\varepsilon = \frac{\sigma_{1it}}{E_{it}} + \left(\frac{\sigma_{1it}}{H_{it}}\right)^{\frac{1}{m_{it}}}, \tag{1}$$

$$\varepsilon = \frac{\sigma_{1ic}}{E_{ic}} + \left(\frac{\sigma_{1ic}}{H_{ic}}\right)^{\frac{1}{m_{ic}}}, \tag{2}$$

where ε is the longitudinal strain, σ_{1it} and σ_{1ic} are the longitudinal stresses in the tension and compression zones, E_{it} and E_{ic} are the moduli of elasticity in the tension and compression, H_{it} and H_{ic} are material constants which include time dependence in tension and compression, respectively, m_{it} and m_{ic} are strain hardening exponents.

The material is functionally graded along the length of the layers. The variations of E_{it} and E_{ic} along the length of layers are given by:

$$E_{it} = E_{it0} e^{\psi_i \frac{x_4}{l}}, \tag{3}$$

$$E_{ic} = E_{ic0} e^{\rho_i \frac{x_4}{l}}, \tag{4}$$

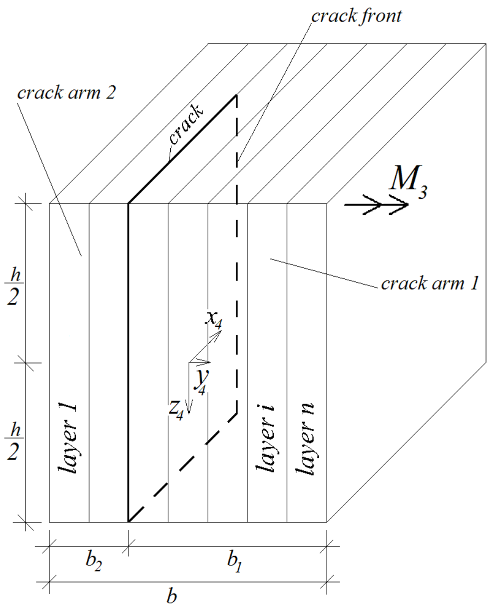

Fig. 1. Beam part with delamination crack front.

where E_{it0} and E_{ic0} are the values of E_{it} and E_{ic} in the left-hand end of the beam, ψ_i and ρ_i are material constants, x_4 is the centroidal axis of the beam ($0 \le x_4 \le l$), l is the beam length.

Due to the non-linear creep behavior, H_{it} and H_{ic} are time dependent [27]:

$$H_{it} = \frac{1}{\left(D_{it} t^{\varphi_{it}}\right)^{1/\delta_{it}}}, \tag{5}$$

$$H_{ic} = \frac{1}{\left(D_{ic} t^{\varphi_{ic}}\right)^{1/\delta_{ic}}}, \tag{6}$$

where D_{it}, φ_{it}, δ_{it} and D_{ic}, φ_{ic}, δ_{ic} are material constants in the tension and compression, respectively, t is time (the values of the exponents, φ_{it} and φ_{ic}, are between zero and unity [27]). The material constants, m_{it} and m_{ic}, which are involved in (1) and (2) are expressed as [27]:

$$m_{it} = \frac{1}{\delta_{it}}, \tag{7}$$

$$m_{ic} = \frac{1}{\delta_{ic}}. \tag{8}$$

It should be mentioned that the first terms of the right-hand sides of equations (1) and (2) treat the instantaneous elastic strain while the non-linear creep is treated by the second terms of the right-hand sides (1) and (2) [27].

The distribution of the strain, ε, that is involved in (1) and (2) is treated by the Bernoulli's hypothesis since beams under consideration have high length to height ratio. Therefore, the strains in the cross-section of delamination arm 1 are distributed linearly:

$$\varepsilon = \kappa_1 \left(z_1 - z_{1n_1}\right), \tag{9}$$

where κ_1 is the curvature, z_1 is the vertical centroidal axis, z_{1n_1} is the coordinate of the neutral axis.

The quantities, κ_1 and z_{1n_1}, are determined by using the equations for equilibrium:

$$N_1 = \sum_{i=1}^{i=n_1} \iint_{(A_{1it})} \sigma_{1it} dA + \sum_{i=1}^{i=n_1} \iint_{(A_{1ic})} \sigma_{1ic} dA, \tag{10}$$

$$M_1 = \sum_{i=1}^{i=n_1} \iint_{(A_{1it})} \sigma_{1it} z_1 dA + \sum_{i=1}^{i=n_1} \iint_{(A_{1ic})} \sigma_{1ic} z_1 dA, \tag{11}$$

where N_1 and M_1 are, respectively, the axial force and the bending moment in delamination arm 1 behind the delamination front ($N_1 = 0$ since the beam is loaded in bending), n_1 is the layers number in delamination arm 1, A_{1it} and A_{1ic} are, respectively, the areas of the tension and compression zones. The stresses, σ_{1it} and σ_{1ic}, have to be obtained in functions of z_1 in order to perform the integration in (10) and (11). However, it is obvious that σ_{it} and σ_{ic} cannot be determined explicitly from the stress-strain relations (1) and (2). Therefore, by using (1), (2) and (9) the coordinate, z_1, is expressed in a function of σ_{1it} and σ_{1ic}. In the tension zone, z_1 is obtained as:

$$z_1 = \frac{1}{\kappa_1}\left[\frac{\sigma_{1it}}{E_{it}} + \left(\frac{\sigma_{1it}}{H_{it}}\right)^{\frac{1}{m_{it}}}\right] + z_{1n_1}. \tag{12}$$

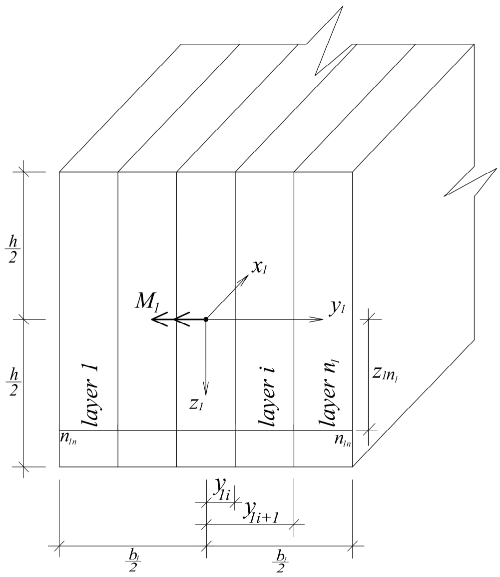

Fig. 2. Cross-section of delamination arm 1 ($n_{1n} - n_{1n}$ is the neutral axis).

In the compression zone, z_1 is found as:

$$z_1 = \frac{1}{\kappa_1}\left[\frac{\sigma_{1ic}}{E_{ic}} + \left(\frac{\sigma_{1ic}}{H_{ic}}\right)^{\frac{1}{m_{ic}}}\right] + z_{1n_1} . \tag{13}$$

By substituting of (12) and (13) in (10) and (11), one arrives at:

$$N_1 = \sum_{i=1}^{i=n_1} \frac{(y_{1i+1} - y_{1i})}{\kappa_1}\left[\frac{\sigma_{1iL}^2}{2E_{it}} + \frac{\sigma_{1iL}^{\frac{1+m_{it}}{m_{it}}}}{(1+m_{it})H_{it}^{\frac{1}{m_{it}}}} - \frac{\sigma_{1iD}^2}{2E_{ic}} - \frac{\sigma_{1iD}^{\frac{1+m_{ic}}{m_{ic}}}}{(1+m_{ic})H_{ic}^{\frac{1}{m_{ic}}}}\right], \tag{14}$$

$$\begin{aligned} M_1 = \sum_{i=1}^{i=n_1} \frac{(y_{1i} - y_{1i+1})}{\kappa_1^2}\Bigg\{ & \frac{\sigma_{1iL}^3}{3E_{it}^2} - \frac{\sigma_{1iD}^3}{3E_{ic}^2} + \frac{m_{it}+1}{(1+2m_{it})E_{it}H_{it}^{\frac{1}{m_{it}}}}\sigma_{1iL}^{\frac{1+2m_{it}}{m_{it}}} - \frac{m_{ic}+1}{(1+2m_{ic})E_{ic}H_{ic}^{\frac{1}{m_{ic}}}}\sigma_{1iD}^{\frac{1+2m_{ic}}{m_{ic}}} + \frac{\sigma_{1iL}^{\frac{2+m_{it}}{m_{it}}}}{(2+m_{it})H_{it}^{\frac{2}{m_{it}}}} - \frac{\sigma_{1iD}^{\frac{2+m_{ic}}{m_{ic}}}}{(2+m_{ic})H_{ic}^{\frac{2}{m_{ic}}}} + \\ & + \frac{\kappa_1 z_{1n_1}\sigma_{1iL}^2}{2E_{it}} - \frac{\kappa_1 z_{1n_1}\sigma_{1iD}^2}{2E_{ic}} + \frac{\kappa_1 z_{1n_1}\sigma_{1iL}^{\frac{1+m_{it}}{m_{it}}}}{H_{it}^{\frac{1}{m_{ti}}}(1+m_{it})} - \frac{\kappa_1 z_{1n_1}\sigma_{1iD}^{\frac{1+m_{ic}}{m_{ic}}}}{H_{ic}^{\frac{1}{m_{ic}}}(1+m_{ic})}\Bigg\}, \end{aligned} \tag{15}$$

where y_{1i} and y_{1i+1} are the coordinates of the lateral surfaces of the layer, σ_{1iD} and σ_{1iL} are the stresses in the upper and the lower surfaces of the layer. There are $2n_1+2$ unknowns, κ_1, z_{1n_1}, σ_{1iD} and σ_{1iL} where $i = 1, 2, ..., n_1$, in equations (14) and (15). Further $2n_1$ equations are composed by using formula (7) and the stress-strain relations (1) and (2):

$$\kappa_1\left(\frac{h}{2} - z_{1n_1}\right) = \frac{\sigma_{1iL}}{E_{it}} + \left(\frac{\sigma_{1iL}}{H_{it}}\right)^{\frac{1}{m_{it}}}, \tag{16}$$

$$\kappa_1\left(-\frac{h}{2} - z_{1n_1}\right) = \frac{\sigma_{1iD}}{E_{ic}} + \left(\frac{\sigma_{1iD}}{H_{ic}}\right)^{\frac{1}{m_{ic}}}, \tag{17}$$

where

$$i = 1, 2, ..., n_1 . \tag{18}$$

Equations (16) and (17) take into account that the lower surface of delamination arm 1 is loaded in tension while the upper surface is in compression (Fig. 2). Equations (14), (15), (16) and (17) are solved with respect to κ_1, z_{1n_1}, σ_{1iD} and σ_{1iL} where $i = 1, 2, ..., n_1$ by the MatLab.

By applying the approach from [22], the TDSERR, G, for the delamination problem shown in Fig. 1 is written as:

$$G = \frac{1}{h}\left(U_1^* + U_2^* - U_3^*\right), \tag{19}$$

Where U_1^*, U_2^* and U_3^* are the time-dependent complementary strain energies (TDCSE) in the cross-sections of the delamination arms 1 and 2 behind the delamination front and in the beam cross-section ahead of the delamination front, respectively.

The quantity, U_1^*, is:

$$U_1^* = \sum_{i=1}^{i=n_1} \iint_{(A_{1it})} u_{01it}^* dA + \sum_{i=1}^{i=n_1} \iint_{(A_{1ic})} u_{01ic}^* dA , \tag{20}$$

where u_{01it}^* and u_{01ic}^* are the time-dependent complementary strain energy densities (TDCSED) in the tension and compression zones of the layer.

The TDCSED in the tension and compression zones are expressed, respectively, as [21]:

$$u_{01it}^* = \frac{\sigma_{1it}^2}{2E_{it}} + \frac{m_{it}\sigma_{1it}^{\frac{1+m_{it}}{m_{it}}}}{(1+m_{it})H_{it}^{\frac{1}{m_{it}}}}, \tag{21}$$

$$u_{01ic}^* = \frac{\sigma_{1ic}^2}{2E_{ic}} + \frac{m_{ic}\sigma_{1ic}^{\frac{1+m_{ic}}{m_{ic}}}}{(1+m_{ic})H_{ic}^{\frac{1}{m_{ic}}}}. \tag{22}$$

By substituting of (12), (13), (21) and (22) in (20), one obtains:

$$U_1^* = \frac{1}{\kappa_1}\sum_{i=1}^{i=n_1}(y_{1i+1} - y_{1i})\left[\frac{\sigma_{1iL}^3}{6E_{it}^2} - \frac{\sigma_{1iD}^3}{6E_{ic}^2} + \frac{m_{it}(3m_{it}+1)\sigma_{1iL}^{\frac{1+2m_{it}}{m_{it}}}}{2(1+2m_{it})(1+m_{it})E_{it}H_{it}^{\frac{1}{m_{it}}}} - \frac{m_{ic}(3m_{ic}+1)\sigma_{1iD}^{\frac{1+2m_{ic}}{m_{ict}}}}{2(1+2m_{ic})(1+m_{ic})E_{ic}H_{ic}^{\frac{1}{m_{ic}}}} + \frac{m_{it}\sigma_{1iL}^{\frac{2+m_{it}}{m_{it}}}}{(1+m_{it})(2+m_{it})H_{it}^{\frac{2}{m_{it}}}} - \frac{m_{ic}\sigma_{1iD}^{\frac{2+m_{ic}}{m_{ic}}}}{(1+m_{ic})(2+m_{ic})H_{ic}^{\frac{2}{m_{ic}}}}\right]. \tag{23}$$

The quantities, U_2^* and U_3^*, can be calculated by performing relevant replacements. In what follows we explain these replacements. For instance, formula (23) is applied also to calculate U_2^*. For this purpose, κ_1, σ_{1iD}, σ_{1iL}, y_{1i}, y_{1i+1} and n_1 are replaced with κ_2, σ_{2iD}, σ_{2iL}, y_{2i}, y_{2i+1} and n_2, respectively, in (23). Equations (14), (15), (16) and (17) are used to determine κ_2 and z_{2n_2}. For this purpose, κ_1, z_{1n_1}, σ_{1iD}, σ_{1iL}, N_1, M_1, y_{1i}, y_{1i+1} and n_1 are replaced with κ_2, z_{2n_2}, σ_{2iD}, σ_{2iL}, N_2, M_2, y_{2i}, y_{2i+1} and n_2, respectively. Here, N_2 and M_2 are the axial force and the bending moment in delamination arm 2 where $N_2 = 0$ because the beam is loaded in bending.

The TDCSE, U_3^*, is obtained by replacing of κ_1, σ_{1iD}, σ_{1iL}, y_{1i}, y_{1i+1} and n_1 with κ_3, σ_{3iD}, σ_{3iL}, y_{3i}, y_{3i+1} and n in formula (21).

The quantities, κ_3 and z_{3n_3}, are found after performing relevant replacements in equations (14), (15), (16) and (17). For instance, after replacing of κ_1, z_{1n_1}, σ_{1iD}, σ_{1iL}, N_1, M_1, y_{1i}, y_{1i+1} and n_1 with κ_3, z_{3n_3}, σ_{3iD}, σ_{3iL}, N_3, M_3, y_{3i}, y_{3i+1} and n, equations (14), (15), (16) and (17) are solved with respect to κ_3, z_{3n_3}, σ_{3iD} and σ_{3iL} by the MatLab.

The general analysis of the TDSERR developed here can be applied at any moment of time because H_{it} and H_{ic} are continuous functions of t.

3. TDSERR in a Multilayered Functionally Graded Beam with a Built-in End

In what follows a particular example that illustrates the utility of the general solution of the TDSERR worked out in section 2 is presented. The example deals with delamination of a multilayered functionally graded beam that is built-in at its right-hand end.

The multilayered beam under consideration is shown in Fig. 3. A delamination of length, a, is located between the layers. The beam has width, b, and height, h. The widths of delamination arms 1 and 2 are b_1 and b_2. The beam is loaded by one bending moment, M, at the free end of delamination arm 1. Apparently, the delamination arm 2 is stress free.

The TDSERR for the delamination problem in Fig. 3 is found by formula (19). The TDCSE, U_1, is obtained by applying (23). Equations (14), (15), (16) and (17) are used to determine κ_1, z_{1n_1}, σ_{1iD} and σ_{1iL} for $M_1 = M$. Since crack arm 2 is free of stresses, U_2 is zero. Formula (22) is applied also to obtain U_3 by replacing of κ_1, σ_{1iD}, σ_{1iL}, y_{1i}, y_{1i+1} and n_1 with κ_3, σ_{3iD}, σ_{3iL}, y_{3i}, y_{3i+1} and n. The quantities, κ_3, σ_{3iD}, σ_{3iL}, y_{3i}, y_{3i+1} and n, are found by equations (14), (15), (16) and (17). For this purpose, κ_1, z_{1n_1}, σ_{1iD}, σ_{1iL}, N_1, M_1, y_{1i}, y_{1i+1} and n_1 are replaced with κ_3, z_{3n_3}, σ_{3iD}, σ_{3iL}, N_3, M_3, y_{3i}, y_{3i+1} and n where $M_3 = M$.

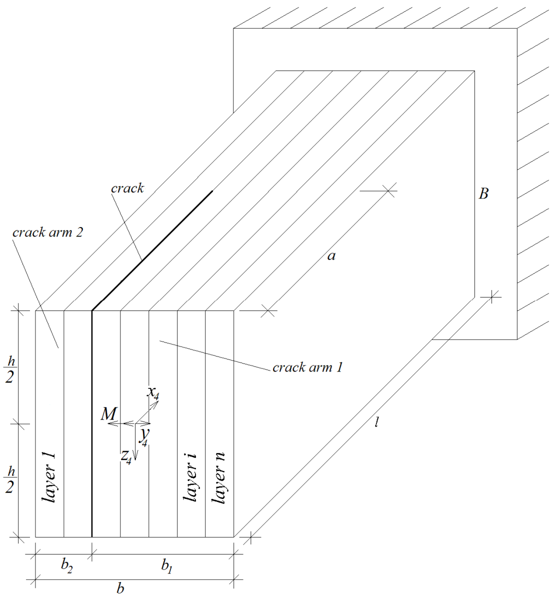

Fig. 3. Multilayered cantilever with a delamination crack.

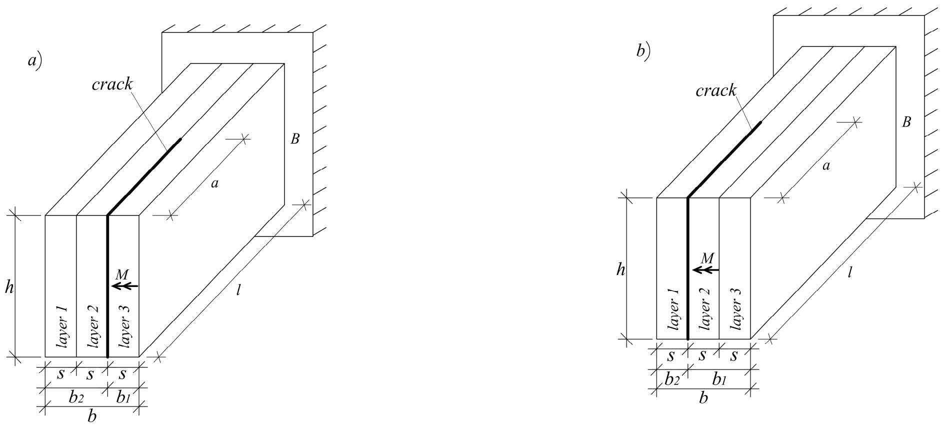

Fig. 4. Cantilever beam delaminated (a) between layers 2 and 3 and (b) between layers 1 and 2.

The TDSERR in the cantilever beam configuration in Fig. 3 is derived also by considering the balance of the energy for verification. The energy balance is written as:

$$M\delta\phi=\frac{\partial U}{\partial a}\delta a+Gh\delta a\ , \tag{24}$$

where the increases of the delamination length and of the angle of rotation of the free end of delamination arm 1 are denoted by δa and $\delta\phi$, U is the time-dependent strain energy (TDSE) cumulated in the beam.

From (22), the TDSERR is obtained as:

$$G=\frac{M}{h}\frac{\partial\phi}{\partial a}-\frac{1}{h}\frac{\partial U}{\partial a}\,. \tag{25}$$

The angle, ϕ, is determined by applying the integrals of Maxwell-Mohr. The result is:

$$\phi=\kappa_1 a+\kappa_3(l-a)\,. \tag{26}$$

The TDSE in the beam is obtained as:

$$U=U_1+U_3\,, \tag{27}$$

where U_1 and U_3 are, respectively, the TDSE in delamination arm 1 and in the un-cracked portion of the cantilever, $a\le x_4\le l$.

The TDSE cumulated in crack arm 1 is written as:

$$U_1=a\sum_{i=1}^{i=n_1}\left(\iint\limits_{(A_{1it})}u_{01it}dA+\iint\limits_{(A_{1ic})}u_{01ic}dA\right), \tag{28}$$

where u_{01it} and u_{01ic} are the time-dependent strain energy densities (TDSED) in the tension and compression zones of layer of delamination arm 1 behind the delamination front.

The quantities, u_{01it} and u_{01ic}, are obtained as [22]:

$$u_{01it}=\frac{\sigma_{1it}^2}{2E_{it}}+\frac{\sigma_{1it}^{\frac{1+m_{it}}{m_{it}}}}{(1+m_{it})H_{it}^{\frac{1}{m_{it}}}}\,, \tag{29}$$

$$u_{01ic}=\frac{\sigma_{1ic}^2}{2E_{ic}}+\frac{\sigma_{1ic}^{\frac{1+m_{ic}}{m_{ic}}}}{(1+m_{ic})H_{ic}^{\frac{1}{m_{ic}}}}\,. \tag{30}$$

By substituting of (29) and (30) in (28), one derives:

$$U_1=\frac{a}{\kappa_1}\sum_{i=1}^{i=n_1}(y_{1i+1}-y_{1i})\left[\frac{\sigma_{1iL}^3}{6E_{it}^2}-\frac{\sigma_{1iD}^3}{6E_{ic}^2}+\frac{(3m_{it}+1)\sigma_{1iL}^{\frac{1+2m_{it}}{m_{it}}}}{2(1+2m_{it})(1+m_{it})E_{it}H_{it}^{\frac{1}{m_{it}}}}-\frac{(3m_{ic}+1)\sigma_{1iD}^{\frac{1+2m_{ic}}{m_{ict}}}}{2(1+2m_{ic})(1+m_{ic})E_{ic}H_{ic}^{\frac{1}{m_{ic}}}}+\frac{\sigma_{1iL}^{\frac{2+m_{it}}{m_{it}}}}{(1+m_{it})(2+m_{it})H_{it}^{\frac{2}{m_{it}}}}-\frac{\sigma_{1iD}^{\frac{2+m_{ic}}{m_{ic}}}}{(1+m_{ic})(2+m_{ic})H_{ic}^{\frac{2}{m_{ic}}}}\right]. \tag{31}$$

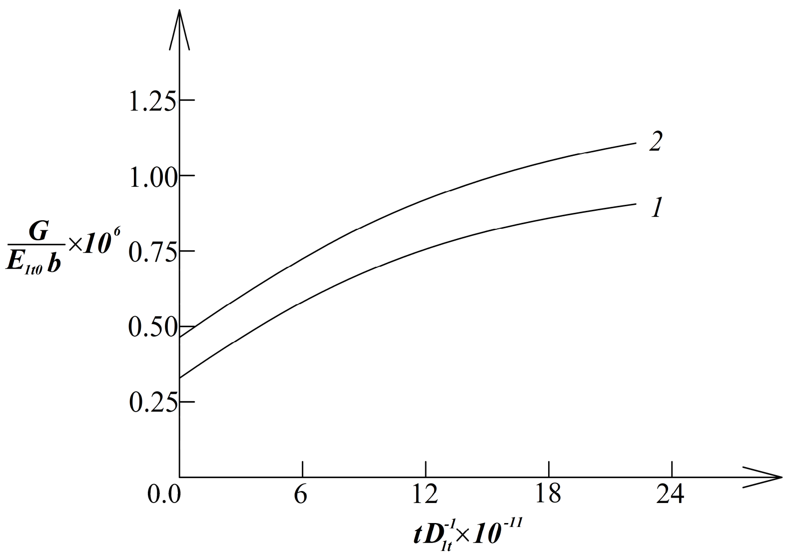

Fig. 5. Variation of the TDSERR with time (curve 1 – for the beam delaminated between layers 1 and 2, and curve 2 - for the beam delaminated between layers 2 and 3).

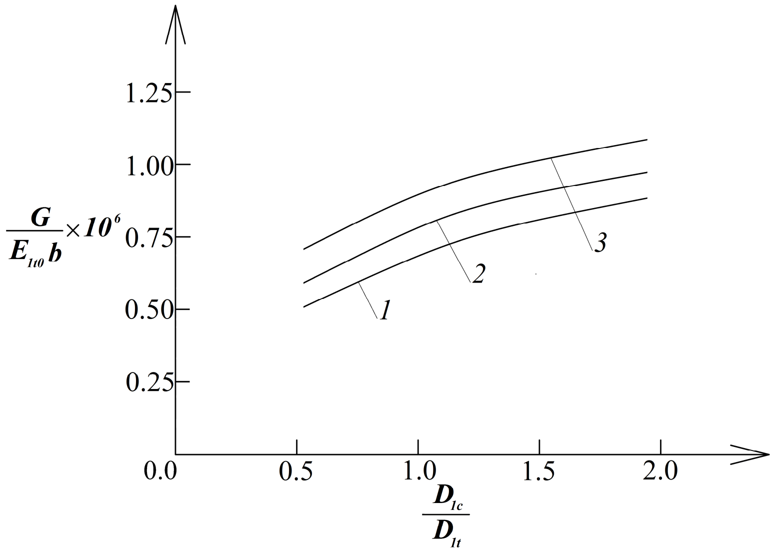

Fig. 6. Variation of the TDSERR with D_{1c} / D_{1t} ratio (curve 1 – for M= 30 Nm, curve 2 – for M= 40 Nm and curve 3 – for M= 50 Nm).

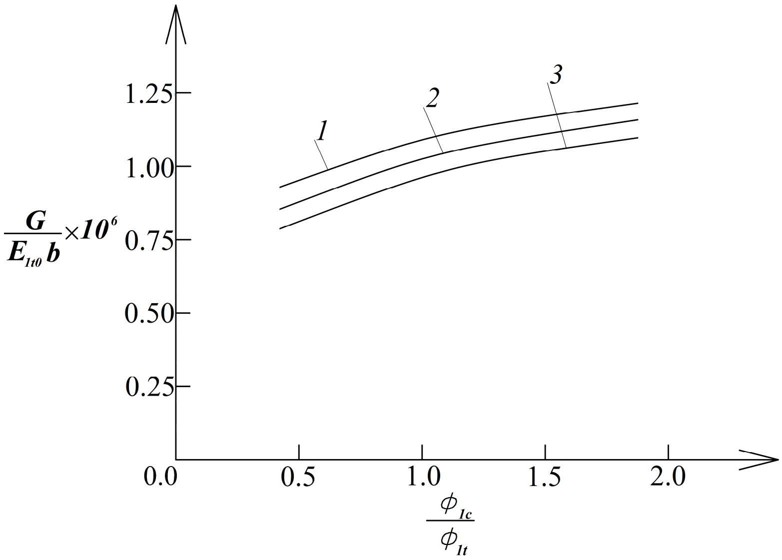

Fig. 7. Variation of the TDSERR with $\varphi_{1c} / \varphi_{1t}$ ratio (curve 1 – at E_{1c0} / E_{1t0}= 0.5, curve 2 – at E_{1c0} / E_{1t0}= 1.0 and curve 3 – at E_{1c0} / E_{1t0}= 2.0).

The TDSE, U_3, in the un-cracked part of the beam is found by replacing of a, κ_1, σ_{1iD}, σ_{1iL}, y_{1i}, y_{1i+1} and n_1, respectively, with $l-a$, κ_3, σ_{3iD}, σ_{3iL}, y_{3i}, y_{3i+1} and n in (31).

It should be mentioned that the TDSERR found by substituting of ϕ and U in (25) matches that found by (17). This fact verifies the delamination analysis of multilayered beams under creep.

4. Numerical Results

The influence of the location of the delamination along the beam width on the TDSERR is examined. Two beam configurations are studied (Fig. 4). The TDSERR is written in normalized form as $G_N = G/(E_{1t0}b)$. A beam delaminated between layers 2 and 3 is depicted in Fig. 4a. A beam delaminated between layers 1 and 2 is also studied (Fig. 4b). The width of each layer in the three-layered beam shown in Fig. 4 is s. Here, s= 0.0025 m, h= 0.010 m and M=50 Nm. The material parameters in the layers are $E_{1t0} = 161000$ MPa, $E_{2t0} = 85000$ MPa, $E_{3t0} = 150000$ MPa, $D_{1t} = 1.58\times10^{-11}$ hours, $D_{2t} = 4.26\times10^{-9}$ hours, $D_{3t} = 2.42\times10^{-6}$ hours, $\delta_{1t} = 4.15$, $\delta_{2t} = 4.05$, $\delta_{3t} = 2.50$, $\varphi_{1t} = 0.40$, $\varphi_{2t} = 0.87$ and $\varphi_{3t} = 0.28$ (the values of material parameters in layers 1, 2 and 3 are for steel, copper and nickel, respectively [27]).

The influence of creep on the delamination behavior is evaluated. For this purpose, the TDSERR in normalized form is plotted against the normalized time in Fig. 5.

From the curves depicted in Fig. 5 one can conclude that the TDSERR increases with the time. This finding is related to the creep and agrees well with previous observations [25] which is a proof for the reliability of the current analysis. It can also be concluded from Fig. 5 that the TDSERR for the beam delaminated between layers 2 and 3 is higher in comparison with that in the beam delaminated between layers 1 and 2. This is attributed to the change in the stiffness of the right-hand delamination arm (the left-hand delamination arm is stress free). Analogical behaviour is observed in previous studies [24] which is a conformation for the correctness of the present solution.

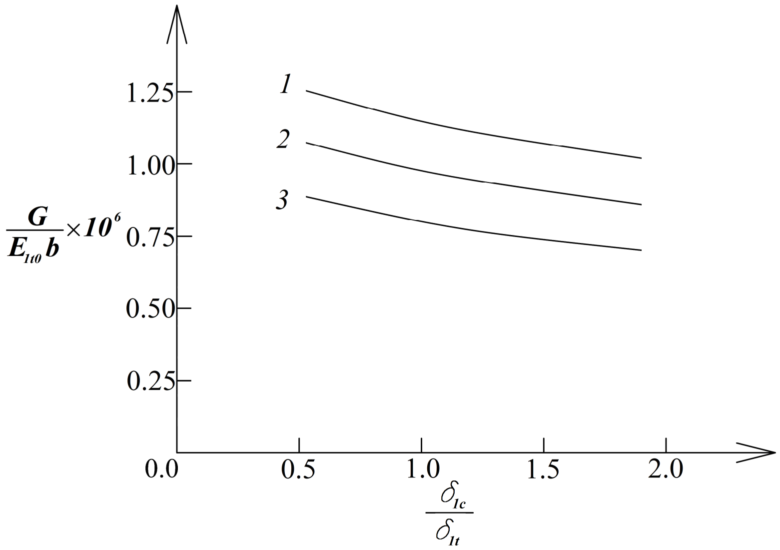

Fig. 8. The variation of the TDSERR with $\delta_{1c} / \delta_{1t}$ ratio (curve 1 – at h / b= 1.3, curve 2 – at h / b= 1.5 and curve 3 – at h / b= 1.7).

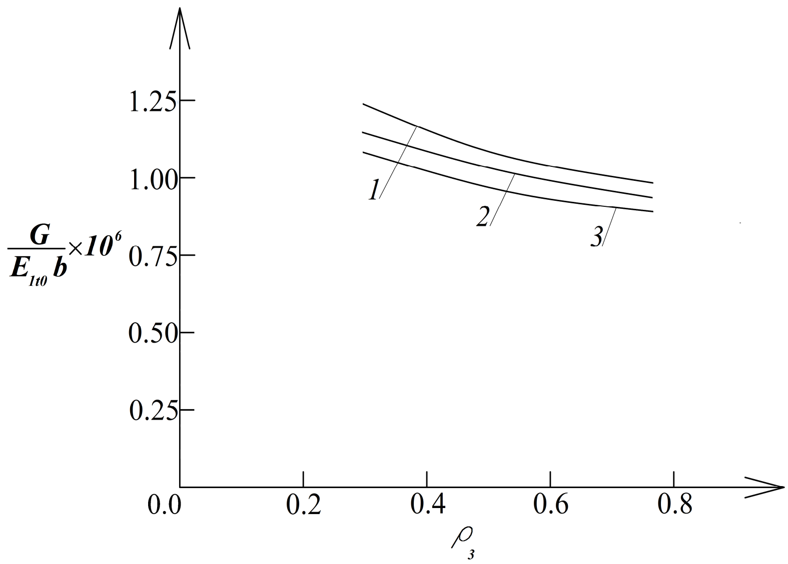

Fig. 9. The variation of the TDSERR with ρ_3 (curve 1 – at $\psi_3 = 0.3$, curve 2 – at $\psi_3 = 0.6$ and curve 3 – at ψ_3= 0.9).

The effect of D_{1c} / D_{1t} ratio on the TDSERR is investigated. The beam delaminated between layers 2 and 3 is considered (Fig. 4a). The variation of the TDSERR with D_{1c} / D_{1t} ratio for three bending moments is examined in Fig. 6. The conclusion that can be drawn from Fig. 6 is that the TDSERR increases with increasing of D_{1c} / D_{1t} ratio. The increase of the bending moment induces increase of the TDSERR (Fig. 6).

In order to study the influence of $\varphi_{1c} / \varphi_{1t}$ ratio, the TDSERR is presented as a function of $\varphi_{1c} / \varphi_{1t}$ ratio in Fig. 7 at three E_{1c0} / E_{1t0} ratios. The beam delaminated between layers 2 and 3 is analyzed. It can be concluded that the TDSERR increases with increasing of $\varphi_{1c} / \varphi_{1t}$ ratio (this observation is explained by decrease of the beam stiffness). Concerning the influence of E_{1c0} / E_{1t0} ratio, it is evident from Fig. 7 that the increase of E_{1c0} / E_{1t0} ratio leads to decrease of the TDSERR (this correlates with previous studies [26] which is an indication for the reliability of the current analysis).

The influence of $\delta_{1c} / \delta_{1t}$ ratio on the delamination is considered too. The beam delaminated between layers 2 and 3 is studied. One can get an idea about the influence of $\delta_{1c} / \delta_{1t}$ ratio on the delamination from Fig. 8 where the variation of the TDSERR with $\delta_{1c} / \delta_{1t}$ ratio is depicted at three h / b ratios. From Fig. 8, one can draw the conclusion that the TDSERR decreases with increasing of $\delta_{1c} / \delta_{1t}$ ratio. The curves in Fig. 8 indicate also that the increase of h / b ratio induces decrease of the TDSERR (this finding is in a good agreement with observations published in [25] which is an indication for the correctness of the current analysis).

The variation of the TDSERR with increase of ψ_3 and ρ_3 is displayed in Fig. 9. It can be seen that the TDSERR reduces when ψ_3 and ρ_3 increase (Fig. 9). The cause for this behaviour is the increase of the beam stiffness.

Concerning the practical usage of the theoretical model presented in this paper, the following should be noticed. In multilayered functionally graded beam structures with delamination under creep, the onset of delamination growth can occur at any value of the external load, if the structure is subjected to loading for a sufficiently long time. Therefore, one of the basic tasks when dealing with such creep delamination problems is to obtain the critical time (the latter is the time at the onset of delamination growth). The present theoretical model can be applied to calculate the critical time for a particular beam configuration with delamination under non-linear creep. For this purpose, the TDSERR has to be calculated by the model at various t and check-up for delamination growth has to be performed by comparing the TDSERR with the fracture toughness. The value of t at which the TDSERR reaches the fracture toughness is the critical time.

5. Conclusion

Delamination in multilayered functionally graded beam configurations was studied in terms of TDSERR assuming different non-linear creep behavior in tension and compression. The analysis of the TDSERR uses the Ramberg-Osgood stress-strain relation. The time dependence induced by the non-linear creep behavior was described by the second term of the Ramberg-Osgood stress-strain relation. General solution of the TDESERR was found. The solution was applied to study delamination of a multilayered functionally graded beam with a built-in end. The TDSERR in the beam under consideration was derived also by analyzing the time-dependent balance of the energy for verification. The study revealed that the non-linear creep induced increase of the TDSERR with time. It was found that increasing of D_{1c} / D_{1t} and $\varphi_{1c} / \varphi_{1t}$ ratios induced also increase of the TDESRR. The increase of E_{1c0} / E_{1t0} and $\delta_{1c} / \delta_{1t}$ ratios induced decrease of the TDSERR. The present paper was a contribution towards the understating of the delamination in multilayered functionally graded materials and structures under non-linear creep. The results obtained in the present study can be useful in structural design of multilayered functionally graded structural members and components subjected to creep when the delamination issue has to be addressed (for instance, the solution can be used to determine the critical time as explained in section 4 of this paper). The limitations of the applicability of the general solution stem from the circumstance that the solution was derived by using the model of prismatic beams whose geometry is characterized by high length to height ratio, i.e. the solution is applicable for beams of high aspect ratio.

Author Contributions

V. Rizov is the only author of this article.

Acknowledgments

Not applicable.

Conflict of Interest

The author declared no potential conflicts of interest with respect to the research, authorship, and publication of this article.

Funding

The author received no financial support for the research, authorship, and publication of this article.

Data Availability Statements

The datasets generated and/or analyzed during the current study are available from the corresponding author on reasonable request.

Nomenclature

A_{1ic}	Area of layer cross-section in compression [m^2]
A_{1it}	Area of layer cross-section in tension [m^2]
a	Delamination length [m]
b	Beam width [m]
D_{ic}	Constant in the time-dependent expression of H_{ic} [hour]
D_{it}	Constant in the time-dependent expression of H_{it} [hour]
E_{ic}	Modulus of elasticity in compression [MPa]
E_{it}	Modulus of elasticity in tension [MPa]
G	Strain energy release rate [MN/m]
H_{ic}	Material constant in Ramberg-Osgood equation which includes time dependence in compression [MPa]
H_{it}	Material constant in Ramberg-Osgood equation which includes time dependence in tension [MPa]
h	Beam height [m]
l	Beam length [m]
M	Bending moment [Nm]
m_{ic}	Strain hardening exponent in Ramberg-Osgood equation in compression [-]
m_{it}	Strain hardening exponent in Ramberg-Osgood equation in tension [-]
N	Axial force [N]
n	Number of layers [-]
n_{1n}	Neutral axis [-]
s	Layer width [m]
t	Time [hour]
U_1	Strain energy [Nm]
u_{01ic}	Strain energy density in compression [N/ m^2]
u_{01it}	Strain energy density in tension [N/ m^2]
x_1	Centroidal axis [m]
y_1	Horizontal centric axis [m]
z_1	Vertical centric axis [m]
z_{1n1}	Neutral axis coordinate [m]
δ_{ic}	Material const. the time-dependent expression of H_{ic} [-]
δ_{it}	Material const. in time-dependent expression of H_{it} [-]
ε	Strain [-]
κ_1	Curvature [m^{-1}]
ρ_i	Material constant controlling the distribution of E_{ic} along the beam length [-]
σ_{ic}	Stress in compression [MPa]
σ_{it}	Stress in tension [MPa]
φ_{ic}	Exponent in the time-dependent expression of H_{ic} [-]
φ_{it}	Exponent in the time-dependent expression of H_{it} [-]
ϕ	Angle of rotation [rad]
ψ_i	Material constant controlling the distribution of E_{it} along the beam length [-]

References

[1] Butcher, R.J., Rousseau, C.E., Tippur, H.V., A functionally graded particulate composite: Measurements and Failure Analysis, *Acta Materialia*, 47(2), 1999, 259-268.
[2] Markworth, A.J., Ramesh, K.S., Parks, Jr.W.P., Review: modeling studies applied to functionally graded materials, *Journal of Materials Science*, 30(3),

1995, 2183-2193.
[3] Kursun, A., Topcu, M., Yücel, U., Stress analysis of a rotating fgm circular disc with exponentially-varying properties, *In: Proceedings of the ASME 2012 International Mechanical Engineering Congress & Exposition IMECE2012*, November 9-15, Houston, Texas, USA, 2012.
[4] Kursun, A., Topcu, M., Thermal Stress Analysis of Functionally Graded Disc with Variable Thickness Due to Linearly Increasing Temperature Load, *Arabian Journal for Science and Engineering*, 38, 2013, 3531–3549.
[5] Kursun, A., Kara, E., Cetin, E., Aksoy, S., Kesimli, A., Mechanical and thermal stresses in functionally graded cylinders, *International Journal of Mechanical, Aerospace, Industrial, Mechatronic and Manufacturing Engineering*, 8(2), 2014, 303-308.
[6] Miyamoto, Y., Kaysser, W.A., Rabin, B.H., Kawasaki, A., Ford, R.G., *Functionally Graded Materials: Design, Processing and Applications*, Kluwer Academic Publishers, Dordrecht/London/Boston, 1999.
[7] Hirai, T., Chen, L., Recent and prospective development of functionally graded materials in Japan, *Materials Science Forum,* 308-311, 1999, 509-514.
[8] Han, X., Xu, Y.G., Lam, K.Y., Material characterization of functionally graded material by means of elastic waves and a progressive-learning neural network, *Composites Science and Technology*, 61(10), 2001, 1401-1411.
[9] Gasik, M.M., Functionally graded materials: bulk processing techniques, *International Journal of Materials and Product Technology*, 39(1-2), 2010, 20-29.
[10] Arda, M., Axial dynamics of functionally graded Rayleigh-Bishop nanorods, *Microsystem Technologies*, 27, 2021, 269–282.
[11] Arda, M., Aydogdu, M., Torsional wave propagation of CNTS via different nonlocal gradient theories, *In: The 23rd International Congress on Sound and Vibration 8ICSV23, Athens (Greece)*, 2016.
[12] Aydogdu, M., Arda, M., Filiz, S., Vibration of axially functionally graded nano rods and beams with a variable nonlocal parameter, *Advances in Nano Research*, 6(3), 2018, 257-278.
[13] Nemat-Allal, M.M., Ata, M.H., Bayoumi, M.R., Khair-Eldeen, W., Powder metallurgical fabrication and microstructural investigations of Aluminum/Steel functionally graded material, *Materials Sciences and Applications*, 2(5), 2011, 1708-1718.
[14] Shrikantha Rao, S., Gangadharan, K.V., Functionally graded composite materials: an overview, *Procedia Materials Science*, 5(1), 2014, 1291-1299.
[15] Wu, X.L., Jiang, P., Chen, L., Zhang, J.F., Yuan, F.P., Zhu, Y.T., Synergetic strengthening by gradient structure, *Materials Research Letters*, 2(1), 2014, 185–191.
[16] Saiyathibrahim, A., Subramaniyan, R. Dhanapl, P., Centrefugally cast functionally graded materials – review, *In: International Conference on Systems, Science, Control, Communications, Engineering and Technology*, 2016.
[17] Mahamood, R.M., Akinlabi, E.T., *Functionally Graded Materials*, Springer, 2017.
[18] Dolgov, N.A., Effect of the elastic modulus of a coating on the serviceability of the substrate-coating system, *Strength of Materials*, 37(2), 2002, 422-431.
[19] Dolgov, N.A., Determination of Stresses in a Two-Layer Coating, *Strength of Materials*, 37(2), 2005, 422-431.
[20] Dolgov, N.A., Analytical Methods to Determine the Stress State in the Substrate–Coating System Under Mechanical Loads, *Strength of Materials*, 48(1), 2016, 658-667.
[21] Hsueh, C.H., Tuan, W.H., Wei, W.C.J., Analyses of steady-state interface fracture of elastic multilayered beams under four-point bending, *Scripta Materialia*, 60, 2009, 721-724.
[22] Hutchinson, J.W., Suo, Z., Mixed mode cracking in layered materials, *Advances in Applied Mechanics,* 64, 1992, 804-810.
[23] Rizov, V.I., Analysis of the Strain Energy Release Rate for a Delamination Crack in a Multilayered Beam with Material Non-Linearity, *IOP Conference Series: Materials Science and Engineering,* 473, 2019, 012002.
[24] Rizov, V.I., Influence of material non-linearity on delamination in multilayered three-point bending beams, *Journal of Theoretical and Applied Mechanics*, 50, 2020, 70-82.
[25] Rizov, V.I., Influence of the viscoelastic material behaviour on the delamination in multilayered beam, *Procedia Structural Integrity*, 25, 2020, 88–100.
[26] Rizov, V.I., Inhomogeneous beams with different behaviour in tension and compression: a longitudinal crack study, *Journal of Applied Mechanics and Technical Physics*, 60, 2019, 908–915.
[27] Dowling, N., *Mechanical Behavior of Materials*, Pearson, 2007.

ORCID iD

Victor Rizov https://orcid.org/0000-0002-0259-3984

How to cite this article: Rizov V. Delamination Analysis of Multilayered Functionally Graded Beams which Exhibit Non-linear Creep Behavior, *J. Appl. Comput. Mech.*, 9(4), 2023, 935–944. https://doi.org/10.22055/jacm.2023.42743.3969